A Wireless and Wearable Body-Pressure-Monitoring System for the Prevention of Pressure-Induced Skin Injuries

Hyunwoo Park, *Student Member, IEEE*, Kyuyoung Kim, Soon-Jae Kweon, *Member, IEEE*, Osman Gul, Jungrak Choi, Yong Suk Oh, Inkyu Park, and Minkyu Je, *Senior Member, IEEE*

***Abstract*—This paper presents a wireless and wearable body-pressure-monitoring system for the on-site, real-time prevention of pressure injuries for immobilized patients. For the prevention of pressure-induced skin injuries, a wearable pressure sensor system is designed to monitor the pressure at multiple sites on the skin and to alert the danger of prolonged application of pressure on the skin with a pressure-time integral (PTI) algorithm. The wearable sensor unit is developed using a pressure sensor based on a liquid metal microchannel and integrated with a flexible printed circuit board that includes a thermistor-type temperature sensor. The wearable sensor unit array is connected to the readout system board for the transmission of measured signals to a mobile device or PC via Bluetooth communication. We evaluate the pressure-sensing performances of the sensor unit and the feasibility of the wireless and wearable body-pressure-monitoring system through an indoor test and a preliminary clinical test at the hospital. It is shown that the presented pressure sensor has high-quality performance with excellent sensitivity to detect both high and low pressure. The proposed system measures the pressure at bony sites on the skin for about six hours continuously without any disconnection or failure, and the PTI-based alarming system operates successfully in the clinical setup. The system measures the pressure applied to the patient and provides meaningful information from the measured data for early diagnosis and prevention of bedsores to doctors, nurses, and healthcare workers.**

***Index Terms*—Wearable device, wireless monitoring system, body pressure monitoring, flexible pressure sensor, liquid-metal-based sensor, temperature sensor, flexible printed circuit board, pressure-time integral, pressure-induced skin injury**

This work was supported by the Ministry of Science and ICT (MSIT), South Korea, through the Institute of Information and Communications Technology Planning and Evaluation (IITP) under Grant 2022-0-00020. *(Hyunwoo Park and Kyuyoung Kim are co-first authors.) (Corresponding authors: Minkyu Je; Inkyu Park.)*

Hyunwoo Park and Minkyu Je are with the School of Electrical Engineering, Korea Advanced Institute of Science and Technology, Daejeon, South Korea (e-mail: hwpark15@kaist.ac.kr; mkje@kaist.ac.kr).

Kyuyoung Kim is with VPIX Medical Inc., Daejeon, South Korea (e-mail: ky.kim@vpixmedical.com).

Soon-Jae Kweon is with the School of Information, Communications and Electronics Engineering, the Catholic University of Korea, Bucheon-si, Gyeonggi-do, South Korea (e-mail: sj.kweon@catholic.ac.kr).

Osman Gul, Jungrak Choi, and Inkyu Park are with the Department of Mechanical Engineering, Korea Advanced Institute of Science and Technology, Daejeon, South Korea (e-mail: osmangul@kaist.ac.kr; cjr1992@kaist.ac.kr; inkyu@kaist.ac.kr).

Yong Suk Oh is with the Department of Mechanical Engineering, Changwon National University, Changwon, South Korea (e-mail: oyongsuk@changwon.ac.kr).

I. Introduction

BODY pressure monitoring plays an important role in healthcare applications as it provides information about body movement, body posture, and pressurized body parts [1]–[4]. Patients who cannot express their intention or control their body by themselves are at risk of bedsores, also known as pressure injuries, which cause pain, discomfort, and secondary infections over bony prominences, as a result of shear, friction, prolonged pressure, and other environmental effects. According to a previous report, 38.8% of pressure injuries occur on the heel (29.7%) and ankle (9.1%) for bedridden patients [5], [6]. Also, it is known that a continuous pressure of about 8 kPa to the skin for about 2 hours can initiate the process of skin damage to bedridden patients, and an increase in temperature at the site of pressure injury accelerates the progress of injury [7]–[9]. To prevent the deterioration of bedsores, continuous and simultaneous body pressure and temperature monitoring is required for areas where pressure injuries are most likely to occur, including sacrum, heel, ischium, ankle, elbow, and others [10]–[12].

Previous approaches to prevent the deterioration of bedsores include avoiding the concentration of pressure in a specific area and monitoring the pressure using a body-pressure-monitoring platform. In [13], a simple air-sitting cushion is designed to disperse the concentrated pressure in a specific skin area. A low-mechanical-modulus structure can help the cushion to cover the bony part softly. In [14], a pneumatic air mattress system is developed to prevent the occurrence and deterioration of bedsores. It applies the pressure on each air cell by an air pump alternatively. These methods disperse the pressure to relieve the pressure on the skin. However, they operate without quantitative measurements of the pressure applied on risky body sites.

To improve this, body-pressure-monitoring systems have recently been developed to quantitatively monitor body pressure while lying on the bed. In [15], using hundreds of arrays of pressure sensors installed on the bed mattress, the body pressure is monitored with a color map. This approach can quantitatively monitor the pressure applied on a large human body area but detects the pressure applied only to the area in contact with the mattress. The pressure on the part of the human body away from the mattress, like the knee and ankle, cannot be monitored using this system. Also, high power consumption and cost are required because the mattress

Fig. 1. Usage concept of the proposed wireless and wearable body-pressure-monitoring system in the clinical environment.

monitors even the parts that are not necessary to be observed to prevent pressure injury. Also, an algorithm to evaluate patients' skin conditions from the quantitively monitored pressure value is not provided.

In this work, a wireless body-pressure-monitoring system using wearable pressure sensors is demonstrated for the on-site monitoring of the pressure applied on bony prominences, where skin injuries are more likely to occur, and the evaluation of patients' skin conditions using an appropriate algorithm.

II. Design and Implementation

There are several requirements to consider thoughtfully in designing a wireless and wearable body-pressure-monitoring system to prevent immobilized patients from pressure injuries. The patient should be comfortable when the device is attached to the patient's body, and it should be convenient for the medical team to attach the device to and detach it from the patient. Also, the pressure sensor should have high sensitivity and accuracy for measuring low-level pressure because the pressure applied to the sensor is distributed as the patient is lying on the bed. There should be no additional pressure caused by the attachment of the device, and the use of wires should be minimized not to make limitations when the medical team changes the patient's body position. Also, the device should be able to measure the pressure on multiple sites to detect skin conditions for various bony prominences on the patient's body.

In this work, a wireless and wearable body-pressure-monitoring system is designed in such a way that all these considerations can be addressed properly. Fig. 1 describes the usage concept of the system in the clinical environment. The wireless and wearable body pressure monitoring system detects the pressure applied to a specific area on the patient's body vulnerable to pressure injuries, estimates the patient's skin condition, and notifies the medical team through an alarm when the skin condition is at risk.

Fig. 2 shows the overall structure of the developed system. The system consists of three functional parts: sensor units, a readout module, and a base station with a pressure-time integral (PTI) algorithm. The sensor unit senses physical signals from the patient. The system has four sensor units,

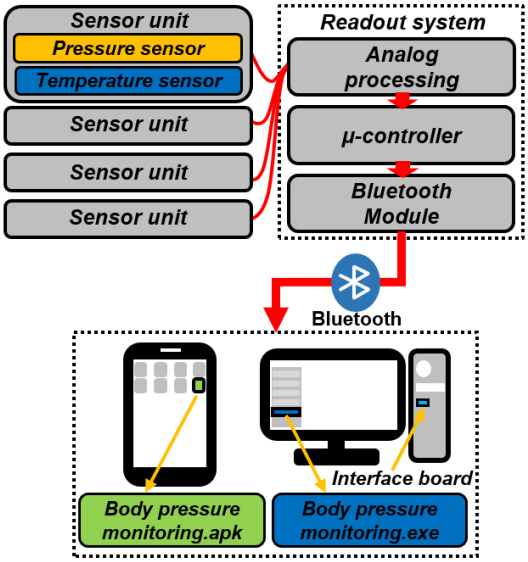

Fig. 2. Overall structure of the developed wireless and wearable body-pressure-monitoring system.

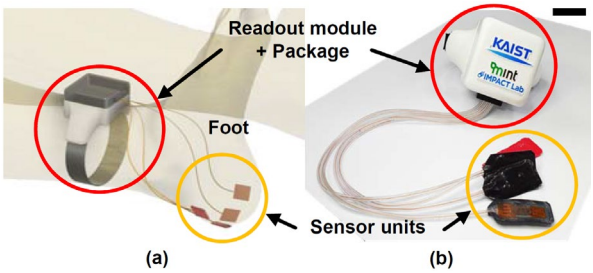

Fig. 3. Wearable body-pressure-monitoring device: (a) conceptual diagram, (b) actual implementation (scale bar = 2 cm).

each with a pressure sensor and a temperature sensor, to concurrently measure eight individual signals in total. The pressure and temperature sensors in each sensor unit transduce changes in the pressure and temperature into changes in their resistances, respectively. All sensor units are packaged with elastic material for flexible and comfortable use. The packaged sensor units cover the sensing areas on the skin smoothly without irritating the skin and generating additional pressure due to the attachment of the sensor unit to the skin. The sensor outputs in the form of resistance are transferred to the readout module. Fig. 3(a) shows the concept of the wearable body-pressure-monitoring device, while Fig. 3(b) shows its actual implementation. In the readout module, the sensor outputs are translated to voltage signals, amplified, and then converted to digital data for wireless transmission to the base station. The PTI algorithm run in the base station converts the digital data from the wearable device to actual pressure values according to pre-characterized fitting curves. Then it accumulates the converted pressure values over time. If the time-accumulated result exceeds a predefined threshold, the system generates an alarm to notify the medical team for timely intervention.

A. Sensor Unit

The proposed sensor unit consists of two sensors: a pressure sensor and a temperature sensor. Since both are resistance-

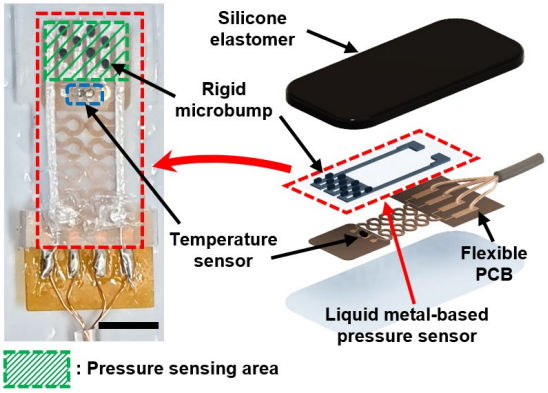

Fig. 4. Implementation and exploded schematic illustration of the proposed sensor unit (scale bar = 5 mm).

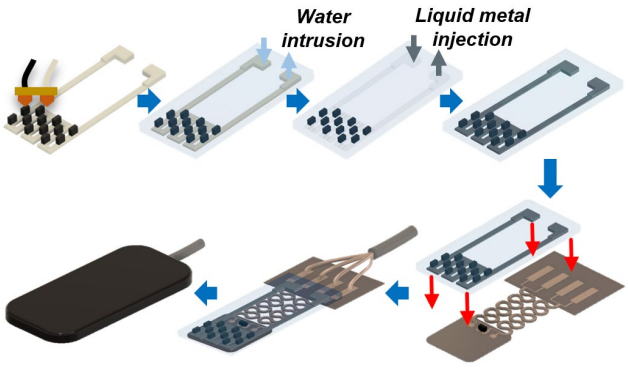

Fig. 5. Components and fabrication process of the proposed sensor unit.

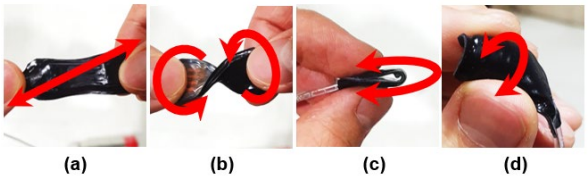

Fig. 6. Sensor unit under various deformation modes: (a) stretching, (b) twisting, (c) folding, and (d) bending.

type sensors, the sensors change their resistance according to the pressure and temperature changes. The pressure sensor is used to sense the pressure applied to the patient's skin and is developed using liquid metal. The temperature sensor is a thermistor used to measure the temperature around the area where the pressure sensor is attached. The used thermistor is a commercial part with a negative temperature coefficient and high sensitivity (NTCG104BH102HT, TDK, Japan).

The sensor units are attached to the patient's body directly, and the quality of signals sensed by the units determines the overall system performance. Therefore, the right material and method should be selected for packaging them so that the sensor units can provide reliable sensing performance and harmless deployment on the patient's skin. Considering the practicability when used by the medical team, the sensor units are attached to the skin using a medical dressing. It is beneficial for its excellent elasticity and air permeability, being friendly in a clinical environment. Silicone (Dragon Skin™ 10, Smooth-On, USA) is employed as a packaging material for the sensor units. Fig. 4 shows the implementation of the packaged sensor unit containing the pressure and temperature sensors.

Recently, liquid-state pressure sensors using ionic liquid and liquid metal have been introduced for wearable electronic devices [16]–[21]. These devices have the advantage of being flexible and stretchable by using liquid electrodes as a sensing material. Also, liquid electrodes are robust against repeated loading and unloading. Liquid-metal-based pressure sensors have high electrical conductivity, negligible vapor pressure at room temperature, self-healing properties, unlimited reversible strain range, and low toxicity [22]–[27]. However, pressure sensors based on liquid metal have difficulties in monitoring a small pressure of a few kPa due to their limited sensitivity. In this work, we employ a microbump-integrated liquid-metal-based soft pressure sensor with high sensitivity [28], [29]. An array of microbumps are introduced to enhance the sensitivity by locally concentrating the deformation of the liquid metal microchannel with negligible hysteresis and excellent stability under cyclic loading. Note that low-level pressure sensing is important in our target application to reliably detect normal conditions where the pressure is well distributed without being concentrated on the patient's bony prominences.

In general, the liquid-metal-based pressure sensor requires an external rigid plate or support structure to ensure its sensing mechanism, mechanical stability, and high sensitivity. While the external rigid plate and support structure prevent the sensing performance change when the sensor is stretched, they make it difficult to measure pressure in the areas with large curvatures, such as bony prominences. To solve this issue, the developed pressure sensor adopts microbumps and a flexible printed circuit board (FPCB). The microbumps are embedded in the fabrication process of the pressure sensor, and they act as the support structure, maintaining the sensor unit flexible.

Fig. 5 shows the components and fabrication process of the sensor unit [28]. The sensor core consists of a microchannel-patterned top layer, a liquid metal microchannel electrode, 3D-printed microbumps, and a bottom layer. The top and bottom layers are fabricated using a stretchable elastomer with an extremely high stretchability and a low elastic modulus. These characteristics are essential because these layers act not only as a substrate for ensuring sensor flexibility but also as an encapsulation layer for preventing liquid metal leakage. Then, a multilayered structure, composed of a sacrificial layer for the microchannel formation and an array of rigid microbumps, is fabricated using a 3D printing process. After the encapsulation of the multilayered structure, the sacrificial layer is selectively removed using water intrusion to produce the microchannel, while the 3D-printed rigid microbumps are monolithically integrated with the microchannel. The empty microchannel is then filled with liquid metal. Lastly, the fine holes for the process of water intrusion and liquid metal injection are filled with the same material as that used in the previous encapsulation process.

A small hole is made below the pressure-sensing area (Fig. 4) so that the SMD-type temperature sensor can measure the temperature of the area where the pressure is measured. The temperature sensor is soldered on the FPCB, acting as the support structure. The fabricated pressure sensor core is

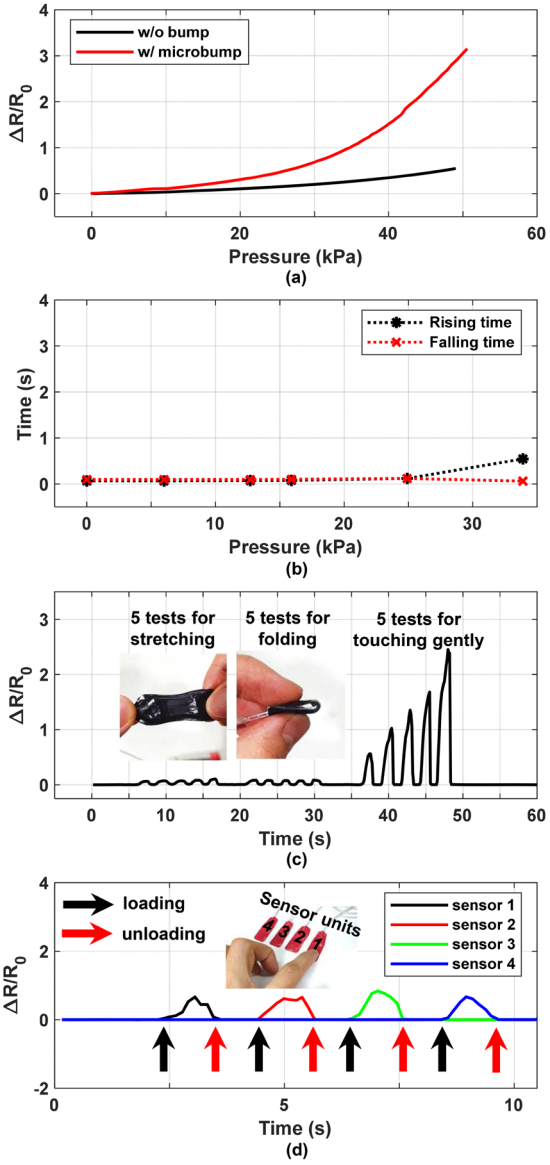

Fig. 7. Measured performances of the pressure sensor: (a) relative resistance change vs. applied pressure, (b) response time for step pressure input, (c) real-time response to five consecutive stretching (30%), folding, and touching events, (d) real-time response to loading and unloading of finger force.

attached to the FPCB, as shown in Fig. 5. The FPCB prevents the device from being stretched except in the pressure-sensing area. On the other hand, the liquid metal electrodes can be stretched as the serpentine electrodes of the FPCB do. Then, the copper pads on the FPCB are connected with electrical wires. Two pads on each side measure the resistance of the pressure sensor, and the other two pads measure the resistance of the thermistor. After all, the pressure sensor integrated with the FPCB is covered with soft top and bottom cases made of silicone to prevent any mechanical failure.

Fig. 6 shows the robustness of the packaged sensor unit under various mechanical deformations of stretching, twisting, folding, and bending. These mechanical characteristics can guarantee high conformality on the skin and adaptability to various human motions while attached.

The performances of the developed pressure sensor are evaluated in terms of normalized resistance change, detection

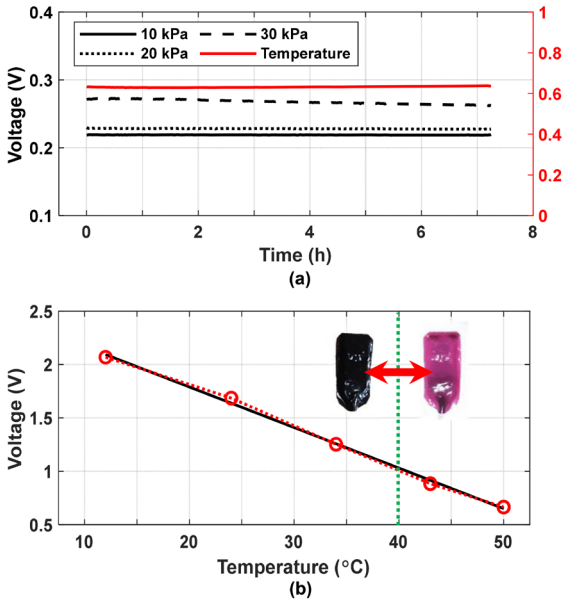

Fig. 8. Additional experiment results of the sensor unit: (a) long-term signal stability under constant pressure (10, 20, and 30 kPa) for over 7 hours, (b) response to temperature change: color change of thermochromic silicone elastomer at the critical temperature, 40 °C.

limit, response time, and dynamic response. Continuous pressure is applied using a universal testing machine (AG-X plus, Shimadzu, Japan) for full loading-unloading cycles. To apply the pressure on the sensing area of the sensor, an acryl cube with a contact area of 10 mm x 10 mm is placed on the sensor. The pressure is applied with a loading speed of 0.3 mm/min, while the corresponding resistance is measured by a source measurement unit (Keithley 2400, Tektronix, USA) with the Kelvin resistance measurement method using four probes. Fig. 7 shows the measurement results. Fig. 7(a) plots the normalized resistance change of the pressure sensor, which is approximately five times higher than that of the typical liquid-metal-based pressure sensor without microbumps at a pressure of 50 kPa.

It is important to measure the pressure and temperature under prolonged static pressure in a wide pressure range for pressure monitoring in the injury-preventing application. As shown in Fig. 8(a), when 10, 20, and 30 kPa of pressure is applied to the sensor unit for over 7 hours, the signals are found to be maintained still without any drift. In addition, the soft silicone covers are colored with thermochromic material, which changes color from black to red when the temperature increases above 40 ºC, as shown in Fig. 8(b). It provides the medical team with a direct visual indication to judge whether the temperature at the sensing area is excessive.

B. Readout Module

The overall block diagram of the readout system board is drawn in Fig. 9. The readout module is designed for converting the pressure and temperature signals sensed by the sensor units to electrical signals and then to digital data, improving the signal quality by signal conditioning, and transmitting the digital data to the base station capable of running the programmed algorithm.

The supply voltage for operating the chips on the board is

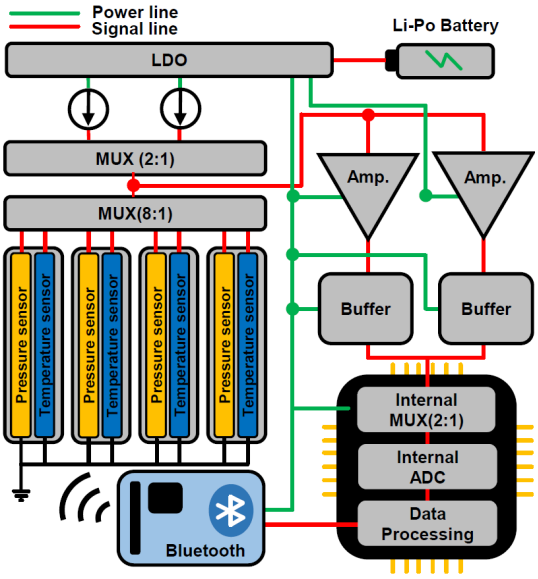

Fig. 9. Overall block diagram of the readout module.

provided by a low-dropout regulator (LDO) chip (TPS73033, Texas Instruments, USA) connected to a Li-Po battery. As explained, the pressure and temperature sensors are resistive sensors, which generate resistance changes corresponding to changes in the pressure and temperature applied to the sensors, respectively. The change in resistance is converted to the voltage signal. There are various methods for converting resistance to voltage. In this design, a simple method of using the current source is adopted. Since the proposed pressure sensor has a very small initial resistance at the level of a few Ω, a method using the voltage source leads to excessive power consumption, and configurations such as a voltage divider and a Wheatstone bridge requiring additional external resistors lead to inaccurate measurement results due to variations in the nominal value of the sensor resistance and mismatches between external resistors used for the configuration.

Therefore, the system is designed to flow well-defined current through the sensors using current sources, directly converting the resistance value to the voltage signal. The voltage signals are in the analog form, and an analog-to-digital converter (ADC) translates them into digital signals for transmission through the wireless communication module. However, the ADC has limitations in its input range. Also, the initial resistances and sensitivities of the pressure and temperature sensors are different from each other. For these reasons, the system is designed by using two current sources capable of delivering the current of different intensities. The LM334 current source chip by Texas Instruments is used in this design. One current source flows a current with a magnitude of 8 mA for the pressure sensor, and the other flows a current of 1.5 mA for the temperature sensor.

For similar reasons, two amplifiers are implemented to amplify the magnitude of the sensed voltage signals, and each of them is designed to have a specific amplification gain determined to fit the characteristics of each sensor. The amplifiers are the noninverting type implemented using the OPA2209 by Texas Instruments.

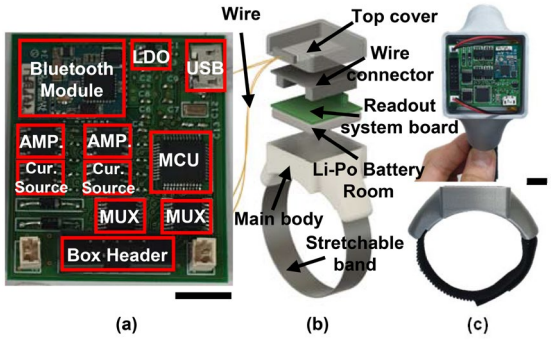

Fig. 10. Implementation of the readout module: (a) system board with all necessary components integrated (scale bar = 1cm), (b) exploded view of the readout module package, (c) actual implementation result (scale bar = 1 cm).

The paths through the current sources, sensors, and amplifiers are formed using two external multiplexers. The multiplexer chip NX3L4051 by NXP is used in this work. The analog voltage signals are fed to the ADC through the internal multiplexer in the microcontroller unit (MCU) and converted to digital data. All the external and internal multiplexers are controlled by the MCU chip ATSAMD21G18A-U by Microchip Technology Inc.

Finally, the converted digital data are transmitted to the base station through Bluetooth communication implemented using a BoT-CLE110 Bluetooth low energy (BLE) module by CHIPSEN. The overall power consumption is 195 mW, and the system can operate for about 7.2 hours when a rechargeable Li-Po battery with a capacity of 380 mAh at 3.7 V is used. Fig. 10(a) shows the fabricated system board and all its components.

For wearable devices, the number of wires used for connecting sensors should be minimized because the wires generate electrical parasitics and their movement distorts sensor signals during the acquisition process. Also, long wires limit the patients' movement and posture. Considering these requirements, the package for the readout module is designed to be placed on the patient's wrist or ankle in a compact size so that the device can be fixed stably and located not far from the sensors. The package comprises several parts – a main body, a stretchable band, a wire connector, a room for the battery, and a top cover. They are 3D-printed using the FDM 3D printer. Fig. 10(b) shows the parts for the readout module, while Fig. 10(c) shows the integrated main body, readout system board, and stretchable band. The package has a form factor of 40 mm x 40 mm x 27 mm.

The main body mechanically supports all the parts for packaging. The stretchable band fits into the groove of the main body, allowing the readout module to be worn on the patient's wrist or ankle comfortably. The main body has room for holding a Li-Po battery, and the developed readout system board is placed on top of the battery. The wire connector is prepared for wires connecting the sensor units and the box header on the readout system board. One tube-type wire bundle comes out from each sensor unit. Two signal lines from the pressure and temperature sensors and one ground line are insulated from each other and contained within the tube.

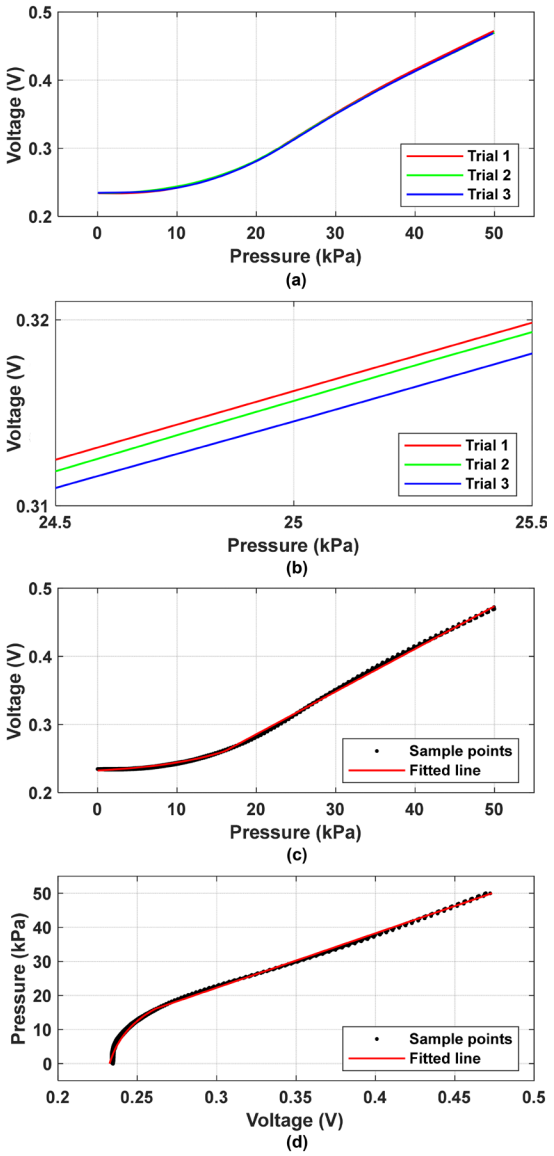

Fig. 11. Measured response of the sensor unit and its fitting curve: (a) response when a continuous pressure from 0 kPa to 50 kPa applied, (b) expanded view of (a), (c) fitting curve of the measured response, (d) inverse function of the fitting curve.

The length of the tube-type wire bundle is 20 cm by default and adjustable from 15 cm to 25 cm by pushing and pulling the wire bundle. It ensures that the sensor units can be stably attached to various body areas requiring pressure monitoring. All the packaging parts are firmly assembled by matching the grooves on each part. The parts can be easily dismantled and reassembled for maintenance.

C. Base Station with Pressure-Time Integral (PTI) Algorithm

In our design, the base station can be selected between two options. One is a smart device like a smartphone or tablet, and the other is a personal computer (PC). When a smart device is employed as the base station, the Bluetooth connection between the smartphone and the BLE module on the board is easily established using the Bluetooth connection protocol built into the smartphone. If a PC is used as the base station, the system additionally needs an interface board to receive the

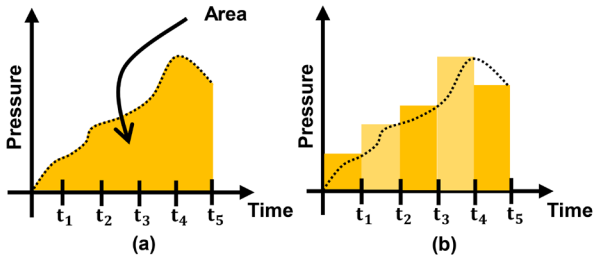

Fig. 12. PTI algorithm: (a) mathematical meaning of the PTI value, (b) actual calculation method to obtain an approximate PTI value.

data using a USB port of the PC. The interface board is implemented using the FT232 USB-UART module and the same BLE module as the one used in the readout module.

The presented sensor units and readout module acquire the pressure data, which should be translated into the actual pressure values at the base station. For this conversion, data fitting is executed for each sensor. While continuous pressure is applied to each sensor unit from 0 kPa to 50 kPa by using the universal testing machine, the response of the sensor unit to the applied pressure is measured. The same experiment is repeated three times to collect sufficient data and prevent the characteristic curve from being overfitted. Fig. 11(a) shows the collected data in voltage, and Fig. 11(b) is the zoomed-in plot obtained by expanding a part of the curves in Fig. 11(a) over the range from 24.5 kPa to 25.5 kPa. Fig. 11(a) proves that the errors between results from repeated measurements are very small, and thus the presented pressure sensor has excellent repeatability.

Although the fitting result may be better when the curve fitting is performed using a high-order polynomial, the result has a high probability of being overfitted. Once overfitted, it is likely that the inverse function for the high-order polynomial curve does not exist. To avoid this problem, the fitting is executed with two base functions: $y = Ae^{Bx} + C$ and $y = Dx + E$. These base functions are chosen intuitively from the data observation. Fig. 11(a) shows that the collected data follow an exponential function when the pressure level is low and then a linear function as the pressure level increases. The data are normalized before data fitting is conducted because the data have large differences between their x-axis values and y-axis values. Fig. 11(c) shows the result of data fitting. Then, the inverse function of the fitting curve is calculated. Fig. 11(d) is the final result used for converting the response of the sensor unit from voltage values to actual pressure values. Once the curve fitting is completed, the coefficients of the fitted curves A, B, C, D, and E are programmed in advance. Then, the conversion from voltage values to pressure values is carried out in a device capable of executing program codes after the voltage data in digital format is transferred through Bluetooth communication.

An algorithm is proposed to calculate a value indicating the possibility of pressure-induced injury occurrence and alarm the medical team when necessary. It is known that pressure injury occurs when excessive pressure is applied to the skin for a prolonged period. Therefore, the PTI value can be a good indicator that quantifies the risk of pressure injury. As shown

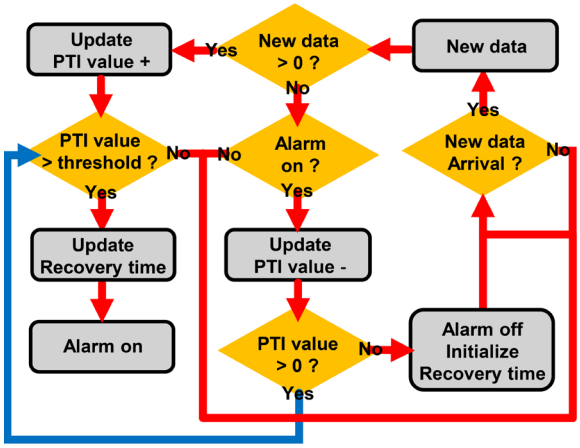

Fig. 13. Flow chart of the PTI algorithm.

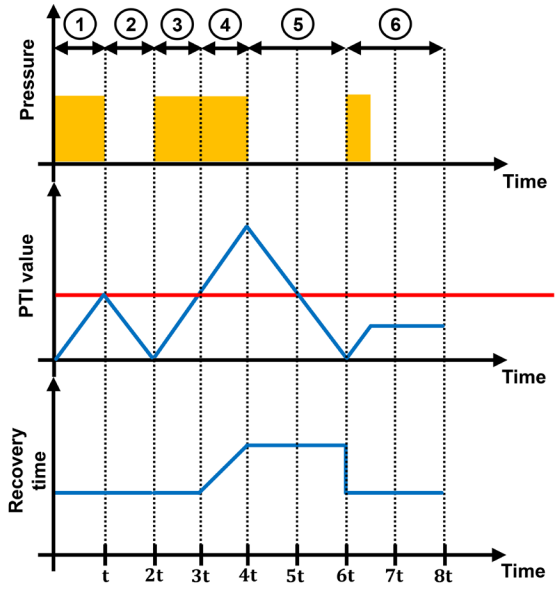

Fig. 14. Example of the operation scenario.

in Fig. 12(a), the PTI value means the area below the pressure-time curve. In practice, the approximate value of the PTI is calculated, as described in Fig. 12(b). The probability of pressure injury occurrence becomes higher as the PTI value increases.

Fig. 13 shows the overall flow chart of the PTI algorithm. The PTI value is updated when the base station device receives a new data sample. If the PTI value exceeds a certain threshold, the algorithm generates an alarm to notify the medical team. However, using a fixed value for thresholding is not reasonable to prevent pressure injuries effectively because the risk of pressure injury significantly depends on various factors such as the patient's environment, weight, and skin condition. Therefore, in our system, the clinician can set different threshold values customized for specific patients and clinical settings.

In the algorithm, another variable, recovery time, is used to indicate the time required for the recovery of the patient's skin from a dangerous condition. If the algorithm generates an alarm, the medical team changes the patient's posture so that the pressure applied to the specific body area can be relieved.

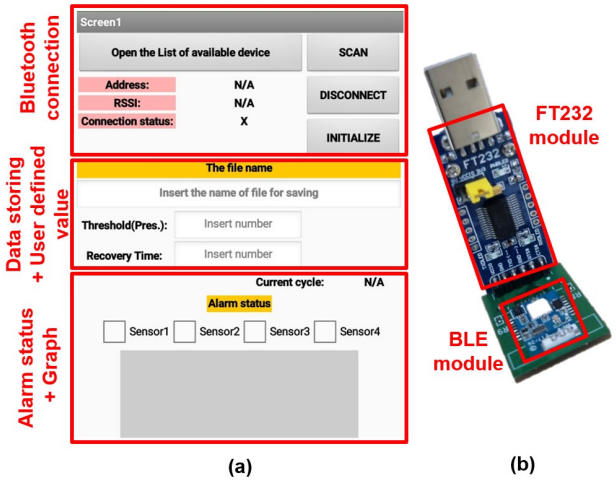

Fig. 15. Implementation of the base station: (a) application software for mobile devices, (b) interface board for PCs.

Once the applied pressure is reduced sufficiently (down to < 0.5 kPa), the algorithm judges that the patient is in a recovery state and decreases the PTI value using a recovery slope calculated as (threshold value) / (initial recovery time value). The initial value of recovery time can also be set differently for different patients and environmental conditions.

Fig. 14 shows an example of scenarios to describe the relationship between the received pressure value, PIT value, and recovery time. For the received pressure values in the top plot of Fig. 14, the PTI value is calculated as shown in the middle plot. In region 1, the PTI value increases over time and reaches the threshold, leading to alarm generation. In region 2, the pressure is removed, and thus the PTI value decreases with the rate determined by the recovery slope. Note that the recovery time does not change from its initial value because the PTI value does not go beyond the threshold. Then, throughout regions 3 and 4, pressure is applied to the patient's body. As a result, the PTI value increases continuously and reaches twice the threshold value in the end. Once the PTI value exceeds the threshold, the recovery time value also increases at the same rate as the PTI value. After the intervention by the medical team, the pressure is removed in region 5, and the PTI value decreases back to zero by the recovery algorithm. The recovery time is also reset to its initial value. Lastly, in region 6, the PTI value increases as much as the pressure is applied. However, no alarm is generated because the PTI value does not reach the threshold. The recovery algorithm is not activated, either.

In our system, the algorithm is executed on mobile devices (e.g., smartphones, tablets) or PCs. Fig. 15 shows the application for mobile devices and the interface board for PCs. The application is developed using a platform, MIT App Inventor. As shown in Fig. 15(a), buttons for establishing a Bluetooth connection are placed in the top section of the graphical user interface (GUI). In the middle section, there are fields to enter the file name for storing raw data and customized values for the threshold and recovery time. In the bottom section, there are checkboxes for sensor units visualizing their alarm on/off status and a display for plotting the measured data. Fig. 15(b) shows the interface board, which

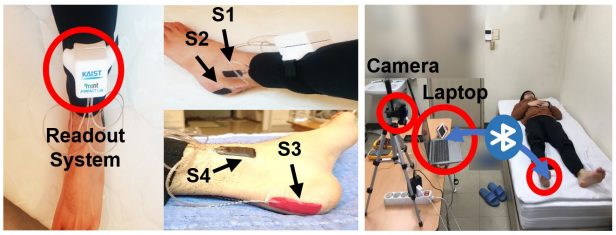

Fig. 16. Setups for preclinical experiment: (a) deployment of the sensor units and readout module, (b) overall settings.

is inserted into the USB port on the PC for establishing a Bluetooth connection.

III. Experiment

To evaluate the performance of the wireless and wearable body-pressure-monitoring system, the experiment is conducted in two different settings. The first experiment is carried out on a normal person in an indoor environment to evaluate the data acquisition performance of the developed system. Then, the experiment in a clinical environment is conducted on a patient to evaluate the overall system performance, including the PTI algorithm. All preclinical and clinical experiments were conducted in accordance with Guidelines issued by the Institutional Review Board at the Eulji Medical Center, Eulji University, Daejeon, South Korea.

A. Preclinical Experiment

The preclinical experiment is conducted when a subject sleeps for about 6 hours. The developed readout module is worn on the subject's leg, and the length of the stretchable band is adjusted for a comfortable fit. Then, the four sensor units are attached to the subject's bony prominences using medical dressing. Fig. 16(a) shows how the readout module and sensor units are deployed. One sensor unit (S1) is attached to the outer ankle, two units (S2 and S3) to the heel, and the other one to the inner ankle (S4). The data is acquired and transferred to the laptop, and the subject's movement is recorded by the camera on the smartphone (Galaxy 9+, Samsung, Korea). In addition, the temperature of the room is recorded with a digital thermometer. Fig. 16(b) shows the overall experimental setup.

All the acquired data are plotted in Fig. 17(a). There are 20 events of changing sleeping posture in total. In Fig. 17(a), the grey dotted lines indicate the time points of posture change. After the initial attachment of sensor units, a large impulsive pressure change is detected when putting the patient's legs on the bed. The monitored data can be categorized into three patterns: supine posture, posture change, and locally concentrated pressure between ankles.

The supine posture data represent that the subject lies upright with the heel and mattress in contact. In the supine posture, the pressure values from the sensor units at the heel (S2 and S3) stay almost constant, and the absolute pressure values are relatively low because the sensors are in contact with the soft surface without a strong impact. The sensor units placed at the other positions (S1 and S4) acquire very low pressure values because

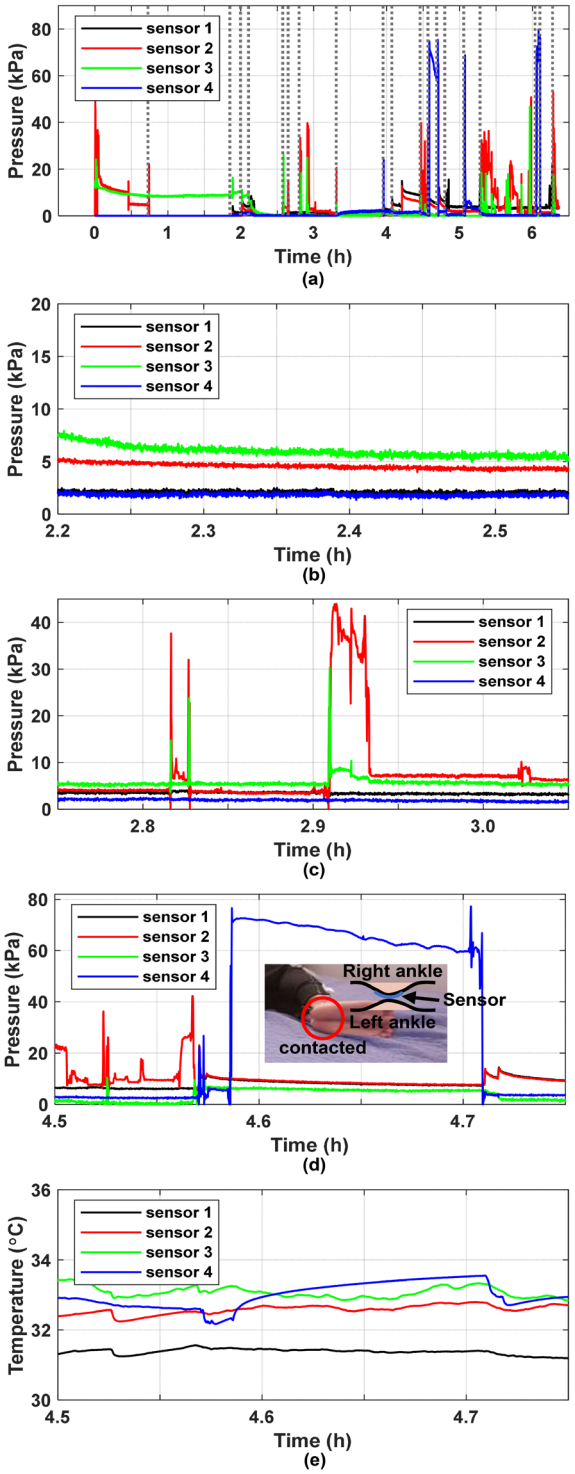

Fig. 17. Preclinical experiment results: (a) all the pressure data measured for 6 hours continuously, (b) pressure data for supine posture, (c) pressure data for posture change, (d) pressure and (e) temperature data for locally concentrated pressure between ankles.

they are not in contact with any surface. Fig. 17(b) shows the pressure values from different sensor units in the supine posture. S2 and S3 acquire relatively constant pressure values below 10 kPa, while the pressure values from S1 and S4 are even lower.

Secondly, the posture change data indicates that the subject suddenly changes the lying posture in various ways, and thus,

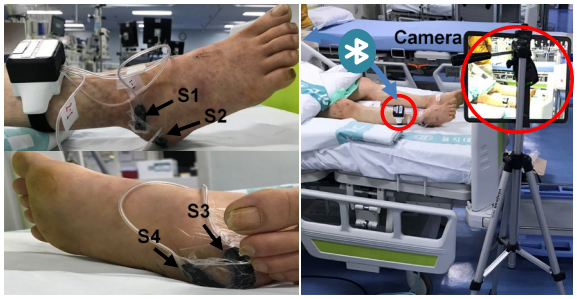

Fig. 18. Setups for clinical experiment: (a) deployment of the sensor units and readout module, (b) overall settings.

dramatic changes in pressure values are detected by sensor units. Fig. 17(c) shows an example of data patterns when a sudden change in posture occurs. When the data is acquired in Fig. 17(c), the subject drops his leg onto the bed. It causes a large impact on the sites that come into contact with the mattress at the instance. Therefore, large increases in pressure values are detected by the sensor units attached to the corresponding sites.

Lastly, when the subject is in a side-lying posture, the inner ankles, which are bony prominences, are sometimes in contact with each other. At that time, the acquired data indicate the pressure locally concentrated at the inner ankle. As shown in Fig. 17(d), the pressure remains at large values of about 60 to 75 kPa. In this posture, the temperature increase is also detected, as shown in Fig. 17(e).

B. Clinical Experiment

The clinical experiment is conducted on an actual patient in the intensive care unit. The patient is awake but cannot make any significant movement by himself. For this experiment, the developed readout module is worn on the patient's leg as in the preclinical experiment. Then, the four sensor units are attached to the patient's bony prominences using medical dressings, as shown in Fig. 18(a). S1 is placed at the outer ankle, S2 at the outer heel, S3 at the inner heel, and S4 at the sole near the heel. The data is acquired for one hour and transferred to the smartphone. All experimental procedures are recorded by the camera on a tablet (Galaxy Tab S5, Samsung, Korea). Fig. 18(b) shows the experimental setup.

All the acquired data are plotted in Fig. 19(a). The pressure is mainly concentrated on the two sensor units, S2 and S4. Fig. 19(b) shows the PTI values calculated from the pressure values acquired by sensor units. The PTI values for S2 and S4 increase rapidly over time, and the value for S2 reaches the threshold after about 47 mins, generating an alarm. Note that a predefined value of 10,000 kPa·s is used for thresholding in this experiment. To prevent the risk of pressure injury, a blanket is put under the patient's calves so that his heels can stay not in contact with the bed. After this intervention, the recovery algorithm decreases the PTI value over time, as shown in Fig. 19(b). The initial value of the recovery time is set to 12,000 s in this experiment. Figs. 19(c) and 19(d) show the posture of the patient's legs and the pressure data before and after the action is taken. It is verified that the developed system with the PTI algorithm can prevent pressure injuries

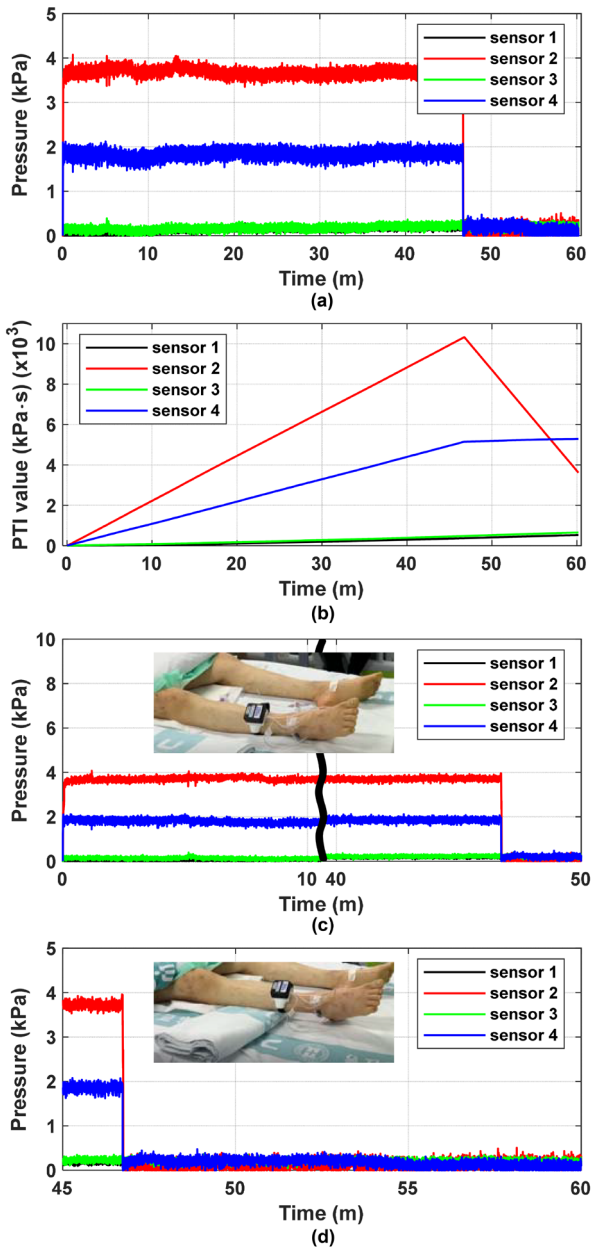

Fig. 19. Clinical experiment results: (a) all the pressure data acquired for 1 hour continuously, (b) PTI value calculated from the acquired pressure data, (c) pressure data and posture before the PTI value reaches the threshold, (d) pressure data and posture after the intervention.

effectively in clinical settings.

IV. Conclusion

The wireless and wearable body-pressure-monitoring system consisting of four sensor units, a readout module, and a PTI algorithm is proposed and implemented. The developed pressure sensors are based on liquid metal and have high sensing performance, self-healing properties, unlimited reversible strain range, and nontoxicity. Using the proposed sensor units and readout module, the pressure and temperature data are continuously acquired from multiple body sites. Then, from the acquired pressure information, the PTI algorithm evaluates the risk of pressure injury occurrence and notifies the

medical team when the estimated risk exceeds a predetermined threshold. The information of pressure applied to a patient's body can be acquired concurrently from 4 different sites and continuously for 7.2 hours through wireless communication when a rechargeable Li-Po battery with a capacity of 380 mAh at 3.7 V is used. Through preclinical and clinical experiments, the successful operation and reliable performance of the developed system are demonstrated, and more importantly, the effectiveness of the system in protecting patients from the risk of pressure-induced injuries.

ACKNOWLEDGMENT

We would like to thank Prof. Hojik Yang at Eulji Medical Center, Eulji University, Daejeon, South Korea, for helping us obtain the preclinical and clinical experiment data.

REFERENCES

[1] S. Han *et al.*, "Battery-free, wireless sensors for full-body pressure and temperature mapping," *Sci. Transl. Med.*, vol. 10, no. 435, p. eaan4950, Apr. 2018.
[2] M. Liu *et al.*, "Large-area all-textile pressure sensors for monitoring human motion and physiological signals," *Adv. Mater.*, vol. 29, no. 41, p. 1703700, Nov. 2017.
[3] C. Gerlach *et al.*, "Printed MWCNT-PDMS-composite pressure sensor system for plantar pressure monitoring in ulcer prevention," *IEEE Sens. J.*, vol. 15, no. 7, pp. 3647–3656, July 2015.
[4] F. Lin A. Wang, Y. Zhuang, M. R. Tomita, and W. Xu, "Smart insole: A wearable sensor device for unobtrusive gait monitoring in daily life," *IEEE Trans. Ind. Inform.*, vol. 12, no. 6, pp. 2281–2291, Dec. 2016.
[5] M. Clark, G. Bours, and T. Delfoor, "Summary report on the prevalence of pressure ulcers," *EPUAP Rev.*, vol. 4, no. 2, pp. 49–57, 2002.
[6] M. Romanelli, M. Clark, G. Cherry, D. Colin, and T. Defloor, *Science and Practice of Pressure Ulcer Management*, 2nd ed., London, United Kingdom: Springer, 2006.
[7] P. K. Vadivu, "Design and development of portable support surface and multilayered fabric cover for bed sore prevention," *Indian J. Surg.*, vol. 77, no. 2, pp. 576–582, Dec. 2015.
[8] G. Matzeu *et al.*, "Skin temperature monitoring by a wireless sensor," in *Proc. Annu. Conf. IEEE Ind. Electron. Soc.*, Nov. 2011, pp. 3533–3535.
[9] S. Ostadabbas, R. Yousefi, M. Faezipour, M. Nourani, and M. Pompeo, "Pressure ulcer prevention: an efficient turning schedule for bed-bound patients," in *Proc. IEEE/NIH Life Sci. Syst. Appl. Workshop*, Apr. 2011, pp. 159–162.
[10] S. A. Shah *et al.,* "Posture recognition to prevent bedsores for multiple patients using leaking coaxial cable," *IEEE Access,* vol. 4, pp. 8065–8072, Nov. 2016.
[11] J. McNeill *et al.*, "Wearable wireless sensor patch for continuous monitoring of skin temperature, pressure, and relative humidity," in *Proc. IEEE Int. Symp. Circuits Syst.*, May 2017.
[12] A. M. Dunk and A Gardner, "The contribution of pressure gradients to advancing understanding of deep tissue injury to sacral regions," *Wound Pract. Res.: J Aust. Wound Manag. Assoc.,* vol. 23, no. 3, pp. 116–122, Sept. 2015.
[13] A. Levy, K. Kopplin, and A. Gefen, "An air-cell-based cushion for pressure ulcer protection remarkably reduces tissue stresses in the seated buttocks with respect to foams: finite element studies," *J. Tissue Viability,* vol. 23, no. 1, pp. 13–23, Feb. 2014.
[14] P. Nair, S. Mathur, R. Bhandare, and G. Narayanan, "Bed sore prevention using pneumatic controls," in *Proc. IEEE Int. Conf. Electron. Comput. Commun. Technol.*, Sept. 2020.
[15] *Body Pressure Mapping on Bed and Mattresses*, novel GmbH, Munich, Germany. [Online]. Available: https://www.novel.de/products/pliance/bed-mattresses/
[16] M.-F. Lin, J. Xiong, J. Wang, K. Parida, and P. S. Lee, "Core-shell nanofiber mats for tactile pressure sensor and nanogenerator applications," *Nano Energy*, vol. 44, pp. 248–255, Feb. 2018.
[17] S. Xu *et al.,* "Biocompatible soft fluidic strain and force sensors for wearable devices," *Adv. Funct. Mater.,* vol. 29, no. 7, p. 1807058, Feb. 2019.
[18] Y. Gao et al., "Wearable microfluidic diaphragm pressure sensor for health and tactile touch monitoring," *Adv. Mater.*, vol. 29, no. 39, Oct. 2017.
[19] X. Yang, Y. Wang, H. Sun, and X. Qing, "A flexible ionic liquid-polyurethane sponge capacitive pressure sensor," *Sens. Actuators A: Phys.,* vol. 285, pp. 67–72, Jan. 2019.
[20] Z. Wang, Y. Si, C. Zhao, D. Yu, W. Wang, and G. Sun, "Flexible and washable poly (ionic liquid) nanofibrous membrane with moisture proof pressure sensing for real-life wearable electronics," *ACS Appl. Mater. Interfaces,* vol. 11, no. 30, pp. 27200–27209, July 2019.
[21] S. G. Yoon and S. T. Chang, "Microfluidic capacitive sensors with ionic liquid electrodes and CNT/PDMS nanocomposites for simultaneous sensing of pressure and temperature," *J. Mater. Chem. C,* vol. 5, no. 8, pp. 1910–1919, 2017.
[22] M. D. Dickey, "Stretchable and soft electronics using liquid metals," *Adv. Mater.,* vol. 29, no. 27, p. 1606425, July 2017.
[23] E. J. Markvicka, M. D. Bartlett, X. Huang, and C. Majidi, "An autonomously electrically self-healing liquid metal–elastomer composite for robust soft-matter robotics and electronics," *Nat. Mater.,* vol. 17, no. 7, pp. 618–624, July 2018.
[24] Y. Lu *et al.*, "Transformable liquid-metal nanomedicine," *Nat. Commun.,* vol. 6, no. 1, p. 10066, Dec. 2015.
[25] C. B. Cooper *et al.*, "Stretchable capacitive sensors of torsion, strain, and touch using double helix liquid metal fibers," *Adv. Funct. Mater.,* vol. 27, no. 20, p. 1605630, May 2017.
[26] T. Jung and S. Yang, "Highly stable liquid metal-based pressure sensor integrated with a microfluidic channel," *Sens.,* vol. 15, no. 5, pp. 11823–11835, May 2015.
[27] Y. Yu, F. Liu, R. Zhang, and J. Liu, "Suspension 3D printing of liquid metal into self-healing hydrogel," *Adv. Mater. Technol.,* vol. 2, no. 11, p. 1700173, Nov. 2017.
[28] K. Kim *et al.*, "Highly sensitive and wearable liquid metal-based pressure sensor for health monitoring applications: integration of a 3D-printed microbump array with the microchannel," *Adv. Healthc. Mater.*, vol. 8, no. 22, p. 1900978, Nov. 2019.
[29] O. Gul *et al.*, "Sensitivity-controllable liquid-metal-based pressure sensor for wearable applications," *ACS Appl. Electron. Mater.*, vol. 3, no. 9, pp. 4027–4036, Aug. 2021.

Hyunwoo Park (Student Member, IEEE) received the B.S. degree in electrical and computer engineering from Ajou University, Suwon, South Korea, in 2014, and the M.S. degree in electrical engineering from Korea Advanced Institute of Science and Technology (KAIST), Daejeon, South Korea, in 2017, where he is currently pursuing the Ph.D. degree in electrical engineering. His research interests include circuits and systems for wireless sensor node, including data processing algorithms.

Kyuyoung Kim received the B.S., M.S., and Ph.D. degree in mechanical engineering from Korea Advanced Institute of Science and Technology (KAIST), Daejeon, South Korea, in 2014, 2016, and 2020 respectively. He is currently CTO in VPIX Medical Inc. His research interests are development of wearable soft sensors and their applications on health monitoring and smart electronic-skin.

Soon-Jae Kweon (Member, IEEE) received the B.S. and Ph.D. degrees in electrical engineering from the Korea Advanced Institute of Science and Technology (KAIST), Daejeon, South Korea, in 2010 and 2018, respectively. He was a post-doctoral researcher with Information Engineering and Electronics Research Institute, KAIST, from 2018 to 2020. After finishing the first post-doctoral research. And he was a post-doctoral researcher with New York University Abu Dhabi, the United Arab Emirates as a post-doctoral associate. He is currently an Assistant Professor with the School of Information, Communications and Electronics Engineering, Catholic University, Bucheon-si, Gyeonggi-do, South Korea. His research aims at designing low-power sensor interface ICs, wireless communication ICs, and data converters for miniature biomedical devices and wireless sensor nodes.

Osman Gul received the B.S. degree in Department of Mechanical Engineering from Korea University, Seoul, South Korea, in 2019, and the M.S. degree in mechanical engineering from Korea Advanced Institute of Science and Technology (KAIST), Daejeon, South Korea, in 2022, where he is currently pursuing the Ph.D. degree in mechanical engineering. His research interests include liquid-metal-based soft sensor and wearable electronics.

Jungrak Choi received the B.S., M.S., and Ph.D. degree in mechanical engineering from Korea Advanced Institute of Science and Technology (KAIST), Daejeon, South Korea, in 2016, 2018, and 2023 respectively. He is currently a post-doctoral researcher with KAIST, South Korea. His research interests are development of 3D electronics and wearable electronics for various applications such as HCI and HRI.

Yong Suk Oh received the B.S., and M.S. degree in mechanical engineering from Pusan National University, Busan, South Korea, in 2007 and 2010 respectively and Ph.D degree in mechanical engineering from Korea Advanced Institute of Science and Technology, Daejeon, South Korea, in 2016.

From 2018 to 2019, he was a postdoctoral fellow at Center for Bio-Integrated Electronics in Rogers research group in Northwestern University, Evanston, IL. He is currently an Assistant Professor with the Department of Mechanical Engineering, Changwon National University, Changwon, South Korea. His research interests included the design and manufacturing of advanced electronics devices based on functional MICRO/NANO structure, and their applications in the field of optoelectronics, robotics, metaverse, healthcare, and smart factory. Dr. Oh was a recipient of the excellent paper award in KAIST in 2016 and the young engineering award in The Korean Society of Manufacturing Process Engineering in 2022.

Inkyu Park received the B.S. degree in mechanical engineering from Korea Advanced Institute of Science and Technology (KAIST), Daejeon, South Korea, in 1998, and the M.S. degree in mechanical engineering from University of Illinois Urbana-Champaign (UIUC), Champaign, IL, USA, in 2003, and the Ph.D. degree in mechanical engineering from University of California, Berkeley (UC Berkeley), Berkeley, CA, USA, in 2007. He has been with the department of mechanical engineering at KAIST since 2009 as a faculty and is currently a full professor, vice department head, and KAIST Endowed Chair Professor. His research interests are nanofabrication, smart sensors for healthcare, environmental and biomedical monitoring, nanomaterial-based sensors and flexible & wearable electronics. He has published more than 165 international journal articles (SCI indexed) and 200 international conference proceeding papers, and holds more than 40 registered domestic and international patents in the area of MEMS/NANO engineering.

Minkyu Je (Senior Member, IEEE) received the M.S. and Ph.D. degrees in electrical engineering and computer science from the Korea Advanced Institute of Science and Technology (KAIST), Daejeon, South Korea, in 1998 and 2003, respectively. In 2003, he joined Samsung Electronics, Giheung, South Korea, as a Senior Engineer and worked on multimode multiband RF transceiver SoCs for GSM/GPRS/EDGE/WCDMA standards. From 2006 to 2013, he was with the Institute of Microelectronics (IME), Agency for Science, Technology and Research (A*STAR), Singapore. He was a Senior Research Engineer from 2006 to 2007, a Member of Technical Staff from 2008 to 2011, a Senior Scientist in 2012, and the Deputy Director in 2013. From 2011 to 2013, he led the Integrated Circuits and Systems Laboratory, IME, as the Department Head. In IME, he led various projects developing low-power 3D accelerometer ASICs for high-end medical motion-sensing applications, readout ASICs for nanowire biosensor arrays detecting DNA/RNA and protein biomarkers for point-of-care diagnostics, ultra-low-power sensor node SoCs for continuous real-time wireless health monitoring, wireless implantable sensor ASICs for medical devices, and low-power radio SoCs and MEMS interface/control SoCs for consumer electronics and industrial applications. He was also the Program Director of NeuroDevices Program under A*STAR Science and Engineering Research Council from 2011 to 2013, and an Adjunct Assistant Professor with the Department of Electrical and Computer Engineering, National University of Singapore, Singapore, from 2010 to 2013. From 2014 to 2015, he was an Associate Professor with the Department of Information and Communication Engineering, Daegu Gyenogbuk Institute of Science and Technology, Daegu, South Korea. Since 2016, he has been an Associate Professor with the School of Electrical Engineering, KAIST. He is the author of five book chapters and has more than 300 peer-reviewed international conference and journal publications in the areas of sensor interface IC, wireless IC, biomedical microsystem, 3D IC, device modeling, and nanoelectronics. He also has more than 50 patents issued or filed. His main research interests include advanced IC platform development including smart sensor interface ICs and ultra-low-power wireless communication ICs, and microsystem integration leveraging the advanced IC platform for emerging applications, such as intelligent miniature biomedical devices, ubiquitous wireless sensor nodes, and future mobile devices. Dr. Je was on the Technical Program Committee and Organizing Committee for various international conferences, symposiums, and workshops, including IEEE International Solid-State Circuits Conference, IEEE Asian Solid-State Circuits Conference, and IEEE Symposium on VLSI Circuits. He is currently a Distinguished Lecturer of IEEE Circuits and Systems Society.